

Axial Crushing of an Aluminum-CFRP Hybrid Component: FE-Modeling, Simulation and Experimental Validation

Sheikh Enamul Hogue¹, Alexander Rauscher²

¹ AIT Austrian Institute of Technology GmbH, Ranshofen, Austria

² University of Applied Sciences Upper Austria, Wels, Austria

Abstract

The crushing performance of aluminum-CFRP (Carbon Fiber-Reinforced Plastics) hybrid generic crash components under axial compression load is experimentally investigated. Aluminum crash components, having similar geometry, are also crushed and compared with the hybrid components. The performance of the hybrid components is found to be twice as much as that of the aluminum components in terms of peak force and specific energy absorption (SEA). Finite element simulations of the crush tests are carried out in LS-DYNA®. The extended 3-parameter Barlat model (MAT36E) is used to characterize the anisotropic elasto-plastic behavior of aluminum sheet. The CFRP laminate is characterized by an orthotropic linear elastic material model (MAT54) with a progressive failure criterion (Chang and Chang). The aluminum-CFRP interface is modeled using tied contact with cohesive mixed mode failure criterion to capture the delamination behavior. Good agreement is found between experiment and simulation in terms of Specific Energy Absorption (SEA) as well as deformation pattern.

1 Introduction

To reduce CO₂ emissions in the automotive and aerospace sector, lightweight optimal design of structures is inevitable. Hence, CFRP is a very interesting material of choice, since it shows high specific stiffness, specific strength and specific energy absorption (SEA) compared to metals [1-2]. However, pure CFRP components have several disadvantages, e.g. catastrophic failure and high production costs [3]. While CFRP absorbs energy mainly by fragmentation and destruction, metallic materials usually absorb energy through plastic deformation [4-6]. Also, metallic materials are more economical than CFRP materials. Hence, a hybrid metal-CFRP component is a potential solution where ductility of metal is combined with high specific stiffness and strength of CFRP.

Research activities on metals combined with CFRPs have been carried out by many researchers in the past [7-10]. However, reliable and predictive numerical simulation of a metal-CFRP hybrid component has always been a challenging task. While various modeling and simulation strategies have been proposed for an accurate crashworthiness simulation of pure CFRP components [11-19], very few literatures can be found on modeling and simulation strategies in metal-CFRP hybrid components [3, 20, 21]. The complexity in modeling and simulation of a metal-CFRP hybrid component can be divided in to three parts: (i) modeling metallic material, (ii) modeling CFRP, (iii) modeling metal-CFRP interface.

LS-DYNA® material model library has an extensive collection of material models for anisotropic sheet metals. In this work, the metallic material (Al-6061T4) of the aluminum-CFRP hybrid component is modeled by MAT36E, an extended version of the Barlat89 model [22]. Several other Barlat and Hill material models (e.g. MAT37, MAT122 and MAT133) are also investigated but not presented in this paper, since they are not capable of describing the material behavior accurately. Barlat_YLD2000 (MAT133) is specifically developed for aluminum sheet. However, the reason behind this model not being able to capture the material behavior accurately could be the lack of available constitutive parameters (e.g. equi-biaxial yield stress, equi-biaxial Lankford co-efficient).

The composite material models in LS-DYNA® can be divided in to two categories: progressive failure models (e.g. MAT22, MAT54/55) and continuum damage mechanics models (e.g. MAT58, MAT158, MAT162) [23]. In this work, the CFRP laminate of the aluminum-CFRP hybrid component is modeled by MAT54. This material model is specifically designed for orthotropic materials such as unidirectional laminates (not fabric). MAT54 is chosen due to two reasons: (i) it is relatively simple and computationally efficient, (ii) it requires minimal input parameters, which means, less coupon tests. However, the model has several non-physical parameters which need to be calibrated by trial and error. In this work, special focus is paid to eliminate these parameters from the material card to reduce the calibration effort.

There are two common approaches for modelling the metal-CFRP interface: cohesive elements, and contact formulations with failure criteria (e.g. tiebreak contacts). The cohesive layer in metal-CFRP hybrid structures is usually very thin. This makes the use of cohesive elements computationally very expensive in explicit FE-simulation. In this work, the aluminum-CFRP interface is modeled by tie-break contact with cohesive mixed mode failure criterion, since it is computationally more efficient. However, the constitutive parameters for cohesive mixed mode failure criterion require additional experiments [24-25] and simulations which is out of the scope of this project. Hence, they are taken from literature [26].

2 Experimental Work

2.1 Material and component

Aluminum sheet EN AW-6061 T4 with 1.0 mm thickness and pre-impregnated UD lamina SIGRAPREG® C U300-0/NF-E420/35% with a nominal cured thickness of 0.28 mm are used for the aluminum-CFRP hybrid generic crash components. Three UD layups at 0°/90°/0° orientation are used. The hybrid components are produced in a subsequent forming (+ curing), cutting and mechanical joining process (Fig.1:). The forming and curing are done at 150°C with a curing duration of 3 minutes. The clamping force is set to 20 kN during forming while the punch velocity is set to 10 mm/s. Seven equidistant M6 screws are used in each side for the mechanical joining. The final geometry had a length of 250 mm and a cross section of approximately 102 mm x 95 mm (without the flange).



Fig.1: Manufacturing steps (from left to right) of the hybrid generic crash element.

Following the same procedure, except without the CFRP layers, aluminum crash components were manufactured (Fig.2:). The aluminum sheet is formed at 150°C temperature at a constant velocity of 10 mm/s while being clamped with a constant force of 20 kN. The formed sheet is kept in the hot forming press for 3 minutes. Finally, seven equidistant M6 screws are used in each side for the mechanical joining.



Fig.2: Generic crash element: (left) aluminum-CFRP hybrid component, (right) aluminum component.

2.2 Crush test

Quasi-static axial crush tests are performed in a vertical configuration at a crosshead velocity of 100 mm/min up to a crushing length of 75 mm. In both types of components, energy absorption by aluminum is done through plastic folding, no significant fracture is observed. In the aluminum-CFRP hybrid component, energy absorption by CFRP layers is done through a complex failure mode (e.g., interlaminar failure, fiber-matrix debonding, fiber pullout, matrix deformation/cracking, fiber breakage), hence, catastrophic failure is observed (Fig.3:).



Fig.3: After crush test: (left & middle) aluminum-CFRP hybrid component, (right) aluminum component.

Five aluminum components and two hybrid components are crushed. The experiments are found to be reproducible in both cases (Fig.4:)(Table 1:).

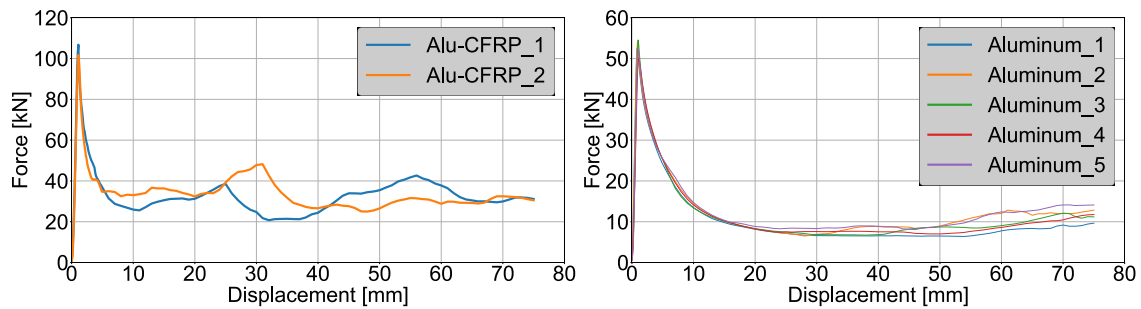


Fig.4: Crush test data: (left) aluminum-CFRP hybrid component; (right) aluminum component.

	Peak Force [kN]	Average Peak Force [kN]	EA [kJ]	Average EA [kJ]	Average SEA [kJ/kg]
Aluminum_1	52.54	52.76	0.76	0.85	2.73
Aluminum_2	54.19		0.90		
Aluminum_3	54.56		0.83		
Aluminum_4	50.13		0.82		
Aluminum_5	52.40		0.93		
Alu-CFRP_1	106.80	104.28	2.45	2.49	5.93
Alu-CFRP_2	101.76		2.53		

Table 1: Crush test data.

The hybrid profiles show significantly higher performance in terms of (average) peak force and (average) specific energy absorption (SEA) (Fig.5:). The average peak force and SEA of the hybrid profiles are at least twice as much as that of the aluminum profiles.

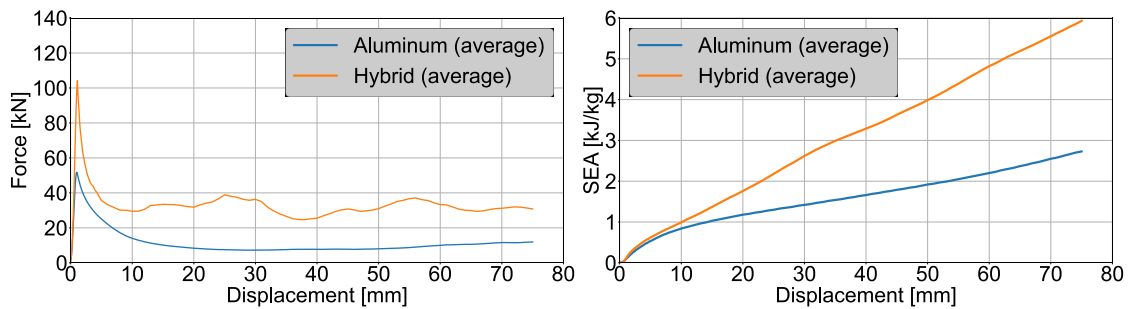


Fig.5: Crush test data (average): aluminum-CFRP hybrid component vs. aluminum component.

3 FE-modeling and simulation

3.1 Material Characterization

The extended 3-parameter Barlat model (MAT36E) is used to characterize the anisotropic elasto-plastic behavior of the aluminum sheet. The hardening curves and the Lankford coefficients in three different directions (at an angle of 0°, 45° and 90° to the rolling direction) of the sheet material are obtained

through standard uniaxial tension experiments. A mild variation of the hardening curves (UT00, UT45, UT90) and the Lankford coefficients (r_{00} , r_{45} , r_{90}) with the angle to the rolling direction is observed (Fig.6:).

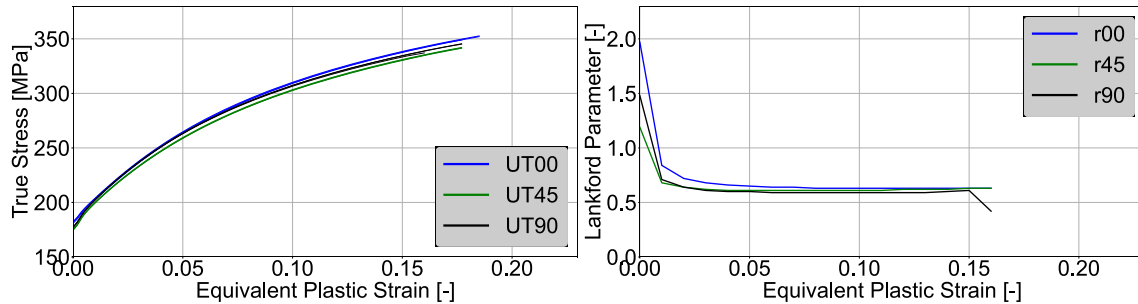


Fig.6: Uniaxial tension test data: hardening up to diffuse necking (left); Lankford parameter (right).

The hardening curves are fitted and extrapolated by mixed Swift and Hockett-Sherby hardening law. An iterative inverse method [27] is followed for calibration.

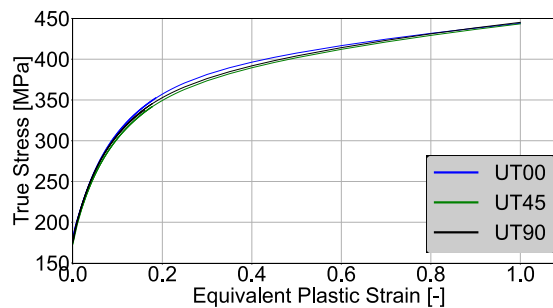


Fig.7: Extrapolated and calibrated hardening curves.

The CFRP laminate is characterized by an orthotropic linear elastic material model (MAT54) with a progressive failure criterion (Chang and Chang). The material parameters are obtained from coupon tests carried out by the material supplier (Table 2:).

Tensile testing	Values	Compression test	Values	Shear test	Values
E-modulus 0°	127 GPa	E-modulus 0°	118.2 GPa	E-modulus	3.4 GPa
Strength 0°	1.97 GPa	Strength 0°	1.43 GPa	Strength	0.055 GPa
Elongation at break 0°	1.5%	Elongation at break 0°	1.4%		
E-modulus 90°	7.8 GPa	E-modulus 90°	7.8 GPa		
Strength 90°	0.048 GPa	Strength 90°	0.17 GPa		
Elongation at break 90°	0.6%	Elongation at break 90°	4.1%		
Poison's ratio 90°	0.03				

Table 2: Coupon test data for SIGRAPREG.

As mentioned earlier, MAT54 has several numerical parameters which cannot be measured experimentally but need to be calibrated by trial and error. In this work, based on an extensive material parameter sensitivity study, only one numerical parameter (SOFT=0.8) is used in addition to the experimentally determined material parameters.

3.2 FE-model

A multi-layer shell approach is followed to model the hybrid crash components where the aluminum sheet and the CFRP laminate are modeled with individual layer of shell elements (Fig.8: left). Each ply within the CFRP laminate is defined by a through thickness integration point. The geometry is meshed using fully integrated quadrilateral shell elements (ELFORM16) of 3 mm x 3 mm size. The component is kept at rest on a rigid plate (Fig.8: right). The plate is constrained in every direction. The loading plate is also modeled as a rigid body (Fig.8: right). Both rigid plates have material parameters (MAT_RIGID) of steel which are used for contact stiffness calculation.

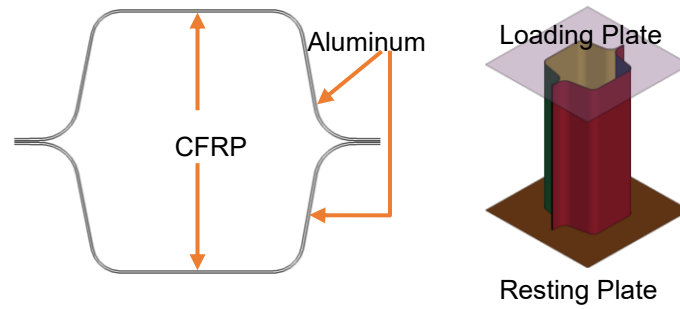


Fig.8: FE-model of the hybrid crash element: (left) top view; (right) isometric view.

Automatic surface to surface contact is defined between the rigid plates and the crash component. The interface between the aluminum and the CFRP layer is modeled using tiebreak contact with a cohesive mixed mode failure criterion. A static coefficient of friction of 0.1 is used based on [21]. A global automatic single surface contact is defined for self-contact mainly for aluminum with a static co-efficient of friction of 1.2 [28]. The bolted joints are modeled using tied contact with no failure. A displacement controlled prescribed motion (rigid) is defined for the loading plate. For computational efficiency, the 75 mm motion was applied in 0.01 second which is 4500 times faster than the real crush test velocity (100 mm/s). This artificial crushing velocity should not have any influence in the simulation result since, no strain rate dependency is calibrated for the material models. Additionally, the kinetic energy due to this artificial velocity is found to be still negligible compared to the internal energy in the model. However, based on simulations using different crushing velocities, the model is found to be sensitive to the crushing velocity, which might be a robustness issue arising from shell element formulation and contact definitions.

The aluminum crash components are modeled following the similar approach in terms of element formulation, mesh size, contact definition. However, a different friction co-efficient (0.61) is used between the rigid plate (loading plate and resting plate both) and the crash component according to [28]. This model is also found to be sensitive to the crushing velocity. The motion of 75 mm for the loading plate is applied in 0.45 s.

4 Results

The simulation results are evaluated in terms of peak force, energy absorption and deformation behavior. With the chosen velocity of the loading plate mentioned in the previous section, the deformation pattern is captured reasonably (Fig.9:).



Fig.9: Deformed shape (simulation and experiment) after crushing: (left) aluminum profile; (right) aluminum-CFRP hybrid profile.

The force-displacement curves match very well for aluminum profile (Fig.10: left). The difference between experiment and simulation in terms of peak force and energy absorption are below 4% (Table 3:).

		Experiment	Simulation	Deviation
Aluminum	Peak force [kN]	52.76	54.61	3.5%
	EA [kJ]	0.85	0.82	-3.5%
Hybrid	Peak force [kN]	104.28	132.44	27%
	EA [kJ]	2.49	2.1	-15.7%

Table 3: Simulation vs. Experiment.

The difference between simulation and experiment for hybrid profiles are relatively higher. The peak force in simulation is overestimated by 27% and the total energy absorption is underestimated by 16%. This significant difference in peak force could be partially coming from the geometrical as well as material imperfection which can not captured in the FE-model. The constitutive parameters for aluminum-CFRP interface failure are taken from literature. This could also be a contributing factor in the difference between experiment and simulation for energy absorption.

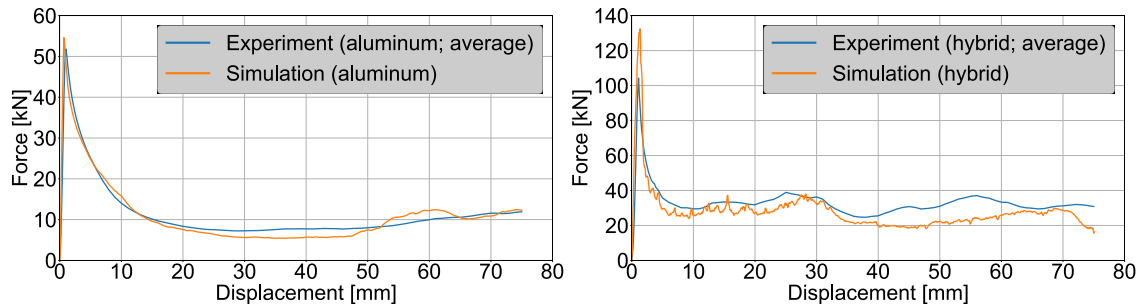


Fig.10: Simulation vs. experiment: (left) aluminum profile; (right) aluminum-CFRP hybrid profile.

5 Summary

First, manufacturing of an aluminum-CFRP hybrid crash component and an aluminum crash component with similar geometry is briefly described. The crush test procedure as well as the results are presented and discussed. The hybrid components are found to be better performing in terms of peak force and energy absorption. Material characterization and the FE-modelling approach are also presented. Finally, the simulation and experimental results are compared and discussed. The simulation results of the aluminum profile are found to be in very good agreement with the experimental results. However, the deviation in simulation from experiment of the hybrid components are relatively higher which clearly indicates the necessity of a more sophisticated material model and detailed modeling approach for such components.

6 Acknowledgement

This work has been partially supported by the European Regional Development Fund (EFRE) in the framework of the EU-program "IWB Investition in Wachstum und Beschäftigung Österreich 2014-2020", and the federal state Upper Austria.

The authors would also like to thank the State of Upper Austria for partial financial support of this research work in the frame of the project PSHero:ER (\#Wi-2020-700757/4-Höf) within the strategic program 'upperVISION2030'.

The support from SGL Carbon with CFRP laminate, coupon test data as well as informative discussions is greatly acknowledged.

7 Literature

- [1] Feraboli P: Development of a Corrugated Test Specimen for Composite Materials Energy Absorption, *Journal of Composite Materials* 42 (3), 2008, 229-256.
- [2] Reuter C, Tröster T: Crashworthiness and numerical simulation of hybrid aluminum-CFRP tubes under axial impact, *Thin-Walled Structures* 117, 2017, 1-9.
- [3] Mildner C: Numerische und experimentelle Untersuchungen des Crashverhaltens von FVK-verstärkten Metallstrukturbauteilen, Technische Universität München, 2012.
- [4] Bardi F C, Yun H D, Kyriakides S: On the axisymmetric progressive crushing of circular tubes under axial compression, *International Journal of Solids and Structures* 40, 2003, 3137-3155.
- [5] Di Paolo B P, Tom J G: A study on an axial crush configuration response of thin-wall steel box components: the quasi-static experiments, *International Journal of Solids and Structures* 43 (25-26), 2006, 7752-7775.
- [6] Ramakrishna S: Microstructural design of composite materials for crashworthy structural applications, *Materials and Design* 18 (3), 1998, 167-173.
- [7] Bambach M R, Elchalakani M, Zhao X L: Composite steel-CFRP SHS tubes under axial impact, *Composite Structures* 87 (3), 2009, 282-292.

- [8] Bambach M R, Elchalakani M: Plastic mechanism analysis of steel SHS strengthened with CFRP under large axial deformation, *Thin-Walled Structure* 45 (2), 2007, 159-170.
- [9] Bambach M R: Axial capacity and crushing of thin-walled metal, fibre-epoxy and composite metal-fiber tubes, *Thin-Walled Structure* 48, 2010, 440-452.
- [10] Song H W, Wan Z M, Xie Z M, Du X W: Axial impact behavior and energy absorption efficiency of composite wrapped metal tubes, *International Journal of Impact Engineering* 24 (4), 2000, 385-401.
- [11] Feindler N: Charakterisierungs- und Simulationsmethodik zum Versagensverhalten energieabsorbierender Faserverbundstrukturen, Technische Universität München, 2012.
- [12] Deleo F, Wade B, Feraboli P, Rassaian M: *Crushing of Composite Structures: Experiment and Simulation*, American Institute of Aeronautics and Astronautics, 2009.
- [13] Sivakumara K, Hopter J, Kopp G, Friedrich H E: Prediction of structural response of FRP composites for conceptual design of vehicles under impact loading. in: *Proceedings of the 8th European LS-DYNA Users Conference*, Strasbourg, 2011.
- [14] Feraboli P, Wade B, Deleo F, Rassaian M, Higgins M, Byar A: LS-DYNA MAT54 modeling of the axial crushing of a composite tape sinusoidal specimen, *Composites: Part A* (42), 2011, 1809-1825.
- [15] Johnson A F: Modelling fabric reinforced composites under impact loads, *Composites Part A: Applied Science and Manufacturing* 32 (9), 2001, 1197-1206.
- [16] Joosten M W, Dutton S, Kelly D et al.: Experimental and numerical investigation of the crushing response of an open section composite energy absorbing element, *Composite Structures* 93, 2011, 682-689.
- [17] Pinho S T, Camanho P P, De Moura M F: Numerical simulation of the crushing process of composite materials, *International Journal of Crashworthiness* 9 (3), 2004, 263-276.
- [18] Chiou L N S, Falzon B G, Boman R et al.: Finite element modelling of composite structures under crushing load, *Composite Structures* 131, 2015, 215-228.
- [19] Xiao X, Botkin M, Johnson N L: Axial crush simulation of braided carbon tubes using MAT58 in LS-Dyna, *Thin-Walled Structures* 47, 2009, 740-749.
- [20] El-Hage H, Mallick P K, Zamani N: Numerical modelling of quasi-static axial crush of square aluminium-composite hybrid tubes, *International Journal of Crashworthiness* 9 (6), 2004, 653-664.
- [21] Reuter C, Tröster T: Crashworthiness and numerical simulation of hybrid aluminium-CFRP tubes under axial impact, *Thin-Walled Structures* 117, 2017, 1-9.
- [22] LS-DYNA Keyword User's Manual, Volume II: Material Models, (r:13191), LS-DYNA R12.
- [23] Wade B: *Capturing the Energy Absorbing Mechanisms of Composite Structures under Crash Loading*, University of Washington, 2014.
- [24] Airbus Industry Standard, Determination of interlaminar fracture toughness energy - Mode I; GIIc-Test., AITM1.0005, 1994.
- [25] Airbus Industry Standard, Determination of interlaminar fracture toughness energy - Mode II; GIIc-Test., AITM1.0006, 1994.
- [26] Ucsnik S: *Development, Experimental and Numerical Investigations of a Novel Metal to Composite Joint Technology*, Technischen Universität Wien, 2013.
- [27] Zhao K, Wang L, Chang Y, Yan J: Identification of post-necking stress-strain curve for sheet metals by inverse method. *Mechanics of Materials* (2016); 92:107-118.
- [28] https://www.engineeringtoolbox.com/friction-coefficients-d_778.html